BULLETIN
OF THE KOREAN CHEMICAL SOCIETY

VOLUME 7, NUMBER 6
DECEMBER 20, 1986

BKCS 7(6) 413-500 (1986)
ISSN 0253-2964

Syntheses and Spectroscopic Studies of $[Cp_2ZrR]_2Fe(CO)_4$

Jaejung Ko

Department of Chemical Education, Korea National University of Education, Chungbuk 320-23

Received June 21, 1986

Hydrocarbon solution of $Cp_2Zr(CH_3)Cl$ react rapidly with $Na_2Fe(CO)_4$ (½ equiv.) to yield $[Cp_2ZrCH_3]_2Fe(CO)_4$ and NaCl. The more soluble metal-metal bonded complex $[Cp_2ZrC_8H_{17}]_2Fe(CO)_2$ has also been prepared through the reaction of $Cp_2Zr(C_8H_{17})BF_4$ and $Na_2Fe(CO)_4$ (½ equiv.). The complexes were characterized by IR, ^1H NMR, ^{13}C NMR, and elemental analysis. The infrared spectrum of $[Cp_2ZrR]_2Fe(CO)_4$ shows four bands, which is indicative of a *cis*-structure. The ^{13}C NMR spectrum provides evidence for the *cis*-structure.

Introduction

For a variety of reasons M-M bonded compounds are the topic of intensive investigation. From the physical side, interest in these systems is largely centered on the unusual structures and bonding. From a chemical standpoint, interest is stimulated by the belief of some chemists that these compounds may possess unusual catalytic properties, and may provide an understanding of supported metal catalysts. This potential is suggested by recent studies revealing bimetallic mechanisms in reactions previously believed to take place at a single metal site.[1]

A systematic entry to metal-metal bonds common in organometallic chemistry consists in metathetic reaction of a metal halogen compound with an anionic metal complex.[2] In a previous paper[3] we reported the syntheses of $Cp_2ZrRFeCp(CO)_2$ through the reaction of Cp_2ZrRCl with strongly nucleophilic metal carbonylate anion $NaCpFe(CO)_2$. The crucial points to be considered in the formation of bimetallic compounds are the nucleophilicity of metal carbonylate anion, leaving group of metal halogen, and solubility of both. By combining these, we could design a route leading to M-M bonded compounds. In this context, it seems reasonable that the selection of stronger nucleophile $Na_2Fe(CO)_4$ instead of $NaFeCp(CO)_2$ and introduction of easy leaving group on zirconium site leads to the syntheses of biheterometallic compounds.

Marks and Newman[4] reported the synthesis of $[Fe(CO)_4MR_2]_2$ made from the reaction of R_2MCl_2 ($R=CH_3$, C_6H_5; M=Ge, Sn) with $Na_2Fe(CO)_4$ known as a supernucleophile. Resen *et. al.*[5] reported a closely related ring supported cluster compound $[Cp_2HfFe(CO)_4]_2$ through the reaction of Cp_2HfCl_2 with $Na_2Fe(CO)_4$. In the light of the reactivity of $Na_2Fe(CO)_4$, it was decided that the reaction of Cp_2ZrRCl with $Na_2Fe(CO)_4$ could lead to direct zirconium-iron metal-metal bonded compounds which are novel and unsupported.

Described herein are the characterization and the syntheses of Zr-Fe bonded complexes formed through the reaction of Cp_2ZrRCl and $Na_2Fe(CO)_4$.

Experimental

All syntheses were done in carefully dried and degassed solvents, under N_2 or in vacuum, and with the use of Schlenk type glassware. All materials were of the highest commercial grade. The Cp_2ZrHCl and $Na_2Fe(CO)_4\cdot$Dioxane were obtained from Aldrich Chemical Co, and the $Cp_2Zr(C_8H_{17})Cl$ was prepared according to literature method.[6] Infrared spectra were measured on a digilab FTS-15B. NMR spectra were measured on a Bruker wp 250. The elemental analyses were performed by Galbraith Labs., Knoxville, TN.

Synthesis of $Cp_2Zr(C_8H_{17})BF_4$. To a stirred benzene solution (20m*l*) of $Cp_2Zr(C_8H_{17})Cl$ (0.9194g) was added $AgBF_4$ dissolved in THF (20m*l*). The reaction was continued for two hours and the mixture was dried under reduced pressure. This was followed by the addition of benzene (30m*l*) to remove the product from AgCl. After filtering AgCl off, the product was dried on a rotary evaporator. The resulting light yellow solid was dried in a vacuum system. Its properties are: M.P: 160-163°C (decomposed); IR (nujol); 1180 (br), 1045 (w), 1014

(m), 916 (m), 814 (s), 724 (m), 730 (vs), 550 (w), 508 (w), ^{1}H NMR ($CDCl_3$); 6.31 (10H), 1.63–0.09 (featureless, 17H) ppm, ^{1}H NMR (d_6-benzene); 6.03 (10H), 1.60–0.09 (featureless, 17H) ppm.

Synthesis of $Fe(CO)_4(Cp_2ZrC_8H_{17})_2$. To a stirred THF solution of $Cp_2Zr(C_8H_{17})BF_4$ (0.405g), one-half this number of moles of $Na_2Fe(CO)_4$ (0.1028g) was added dropwise at −78°C The reaction temperature was increased to 0°C and the reaction was continued for one hour. After stripping the solvent off, the product was heated at 40°C on a vacuum line in order to remove THF of solvation. A minimum amount of THF (5m*l*) was then added to it. After filtration, the solvent was stripped off. Benzene (10–15m*l*) was added to the resulting violet solid, and the solution was filtered. After removal of solvent, the product was dried in a vacuum system. The properties are: M.P.; 114–117°C, IR (in cyclohexane); 2046, 2022, 1995, and 1965 cm^{-1}, ^{1}H NMR (d_6-benzene); 5.92 (10H), 1.31 (28H), 0.97 (6H); Elemental analysis; C, 56.70 (cal. 57.39); H, 5.85 (cal. 6.45); Fe, 6.46 (6.69).

Synthesis of $Fe(CO)_4(Cp_2ZrCH_3)_2$. To a stirred THF solution of two equimolar of $Cp_2Zr(CH_3)Cl$ (0.496g) was added an equimolar amount of $Na_2Fe(CO)_4$ (0.365g) at room temperature. The reaction was continued for two hours. The solution changed from dark red to light brown. After filtering it in order to remove NaCl, the resulting THF solution was stripped of THF at reduced pressure. To that solid a minimum amount of benzene was added, and the mixture was filtered. The resulting dark brown solid was washed with cyclohexane three times (each 30m*l*) to remove remaining $Cp_2Zr(CH_3)Cl$, followed by washing with use of a minimum amount of benzene. The solution was pumped off and dried in a vacuum system. The properties are: M.P.; 121–125°C (decomposed), IR (nujol); 2030, 1962, 1946, and 1938 cm^{-1}. ^{1}H NMR (d_6-benzene); 5.78 (10H), 0.59 (6H) ppm; elemental analysis; Fe, 8.84 (cal. 8.72), C, 50.02 (cal. 48.74) H, 4.27 (cal. 4.06).

^{13}CO enrichment of $Fe(CO)_4\{ZrCp_2(C_8H_{17})\}_2$. $Fe(CO)_4\{ZrCp_2(C_8H_{17})\}_2$ (0.35g) and n-hexane were placed in a quartz flask. The flask was connected to a vacuum line. The flask was cooled at liquid nitrogen temperature and charged with ^{13}CO (760 mmHg). Ultraviolet irradiation from a 140-w lamp resulted in exchange and irradiation was continued for 4 hours. The progress was monitored by infrared spectroscopy.

Results and Discussion

The reaction of two equivalent of $Cp_2Zr(R)X$ with $Na_2Fe(CO)_4$ results in the formation of the zirconium–iron bonded complexes **1** and **2**, respectively, in high yields (eq. 1).

$$2Cp_2ZrRX + Na_2Fe(CO)_4 \rightarrow Fe(CO)_4[Cp_2ZrR]_2 + 2NaCl$$

1 R = CH_3, X = Cl

2 R = C_8H_{17}, X = BF_4

Initially we attempted to form zirconium–iron bonded complex through the reaction of $Cp_2Zr(C_8H_{17})Cl$ with $Na_2Fe(CO)_4$. Unfortunately this reaction did not lead to $Fe(CO)_4[Cp_2Zr(C_8H_{17})]_2$. We sought to determine if $(Cp_2ZrR)_2$ $Fe(CO)_4$ species could be prepared by substituting a good leaving group for Cl. BF_4 introduced at a zirconium site has been found to be an excellent leaving group. The structures of compounds prepared in this way were deduced from their IR, ^{1}H NMR, ^{13}C NMR spectra and elemental analyses.

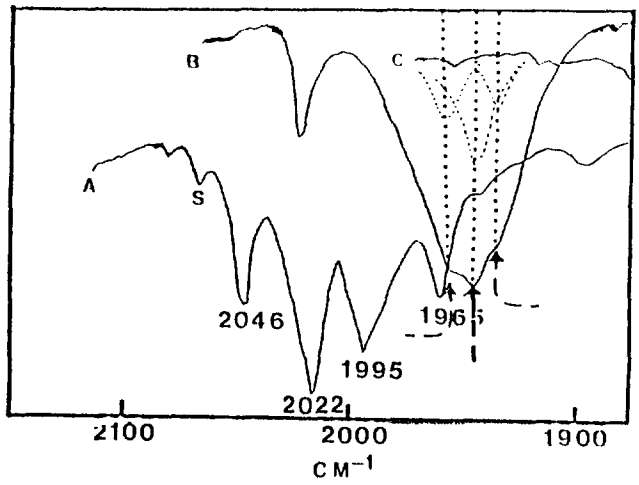

Figure 1. A. The ν(CO) region of the infrared spectrum of $Fe(CO)_4\{Cp_2Zr(C_8H_{17})\}_2$ in cyclohexane solution. B. The ν(CO) region of the infrared spectrum of $Fe(CO)_4\{Cp_2Zr(CH_3)\}_2$ on a nujol mull. C. The ν(CO) region of the infrared spectrum of $Na_2Fe(CO)_4$ in THF solution.

Infrared spectroscopy is useful for understanding *cis*- and *trans*-disubstituted carbonyls, $M(CO)_4L_2$ involving $Fe(CO)_4^{2-}$. In a *cis*-disubstituted compound (A), group theory[7] leads us to expect four IR-active bands since the symmetry about the central metal is effectively C_{2v}, and the CO vibrations span the representation $2a_1 + b_1 + b_2$.

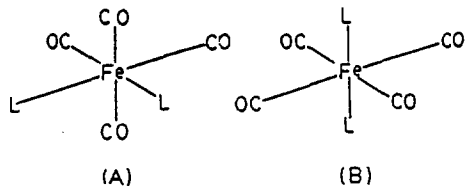

In a type (B), group theory tells us that there is only one infrared active species, ν(CO) mode, e_u, for these complexes of D_{4h} symmetry. In this sense, the numbers of a characteristic CO stretching modes in the carbonyl region are quite helpful in determining whether a *cis*- or *trans*-disubstituted compound is present.

The infrared spectrum of $Fe(CO)_4(Cp_2ZrR)_2$ is shown in Figure I along with that of the starting material $Na_2Fe(CO)_4$ which has one broad peak at 1788 cm^{-1} due to the anion $Fe(CO)_4^{2-}$. In both compounds (R = CH_3, C_8H_{17}), there are four well-separated bands. These bands are shifted to higher frequency than those of the anion $Fe(CO)_4^{2-}$. This indicates that the reaction resulted in the formation of a neutral species. Four bands at 2046, 1022, 1995, and 1965 cm^{-1} of compound $Fe(CO)_4[Cp_2Zr(C_8H_{17})]$ taken in cyclohexane are clearly indicative of a *cis*-structure about the iron center of the zirconium moieties. Similar patterns were observed in $Fe(CO)_4(SiMe_2CH_2CH_2\ SiMe_2)$,[8] $Fe(CO)_4(SiMe_3)_2$,[9] $Fe(CO)_4$ $(CF_2CF_2H)_2$,[10] $Fe(CO)_4(HgBr)_2$,[11] or $OS(CO)_4(SiMe_3)_2$.[12] The infrared spectrum of $Fe(CO)_4(Cp_2ZrCH_3)_2$ taken on nujol mull shows two strong bands, 2030 and 1946 cm^{-1}, with shoulders at 1958 cm^{-1} and 1938 cm^{-1}. When these compounds are compared

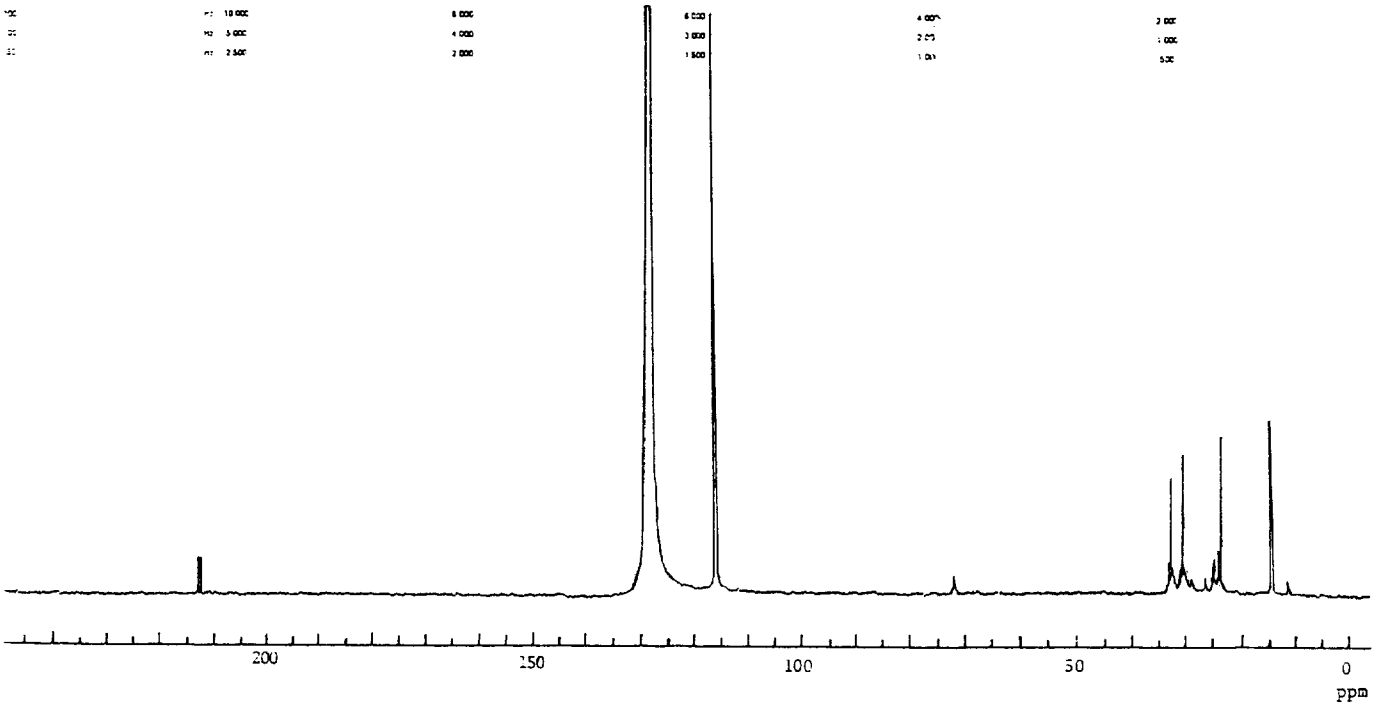

Figure 2. ^{13}C NMR Spectrum of $Fe(CO)_4[Cp_2ZrC_8H_{17}]_2$.

with that of $Fe(CO)_4(Cp_2ZrCl)_2$,[13] which shows one major peak at 1970 cm^{-1}, the structure of both compounds clearly is seen to be *cis*-substituted compound (1)

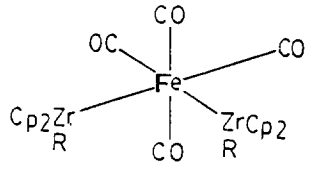

(I)

The main cause of the difference in structural geometry between $Fe(CO)_4(Cp_2ZrCl)_2$ and $Fe(CO)_2(Cp_2ZrR)_2$ is not clear, but presumably it is due to electronic effects rather than steric hindrance. Four CO stretching bands of these compounds are clearly indicative of a *cis*-substituted structure. The positions of the bands associated with the carbonyl stretching vibration are higher than those observed in iron pentacarbonyl, although this is in agreement with the concept of higher formal charge on the iron group. The change in stereochemistry and effects of substituents are probably more significant in accounting for this small variation in energy. The spectrum observed for the compound of $Fe(CO)_4[Cp_2Zr(C_8H_{17})]_2$ in the solid state, in nujol mull, was more complex and showed six bands at 2037, 2032, 2016, 1990, 1987 and 1956 cm^{-1}. It may be related to the existence in the solid of more than one of the geometric isomers or to solid-state splitting. In contrast, the solution spectrum of $Fe(CO)_4[Cp_2Zr(C_8H_{17})]_2$ was consistent with the presence of only one major isomer obeying the C_{2v} selection rules for the carbonyl groups in the molecule.

The ^1H NMR spectrum of the compound $Fe(CO)_4(Cp_2ZrC_8H_{17})_2$ shows three peaks. The peaks at 5.92 ppm, 1.31 ppm and 0.97 ppm are assigned to the Cp, methylene and CH_3 groups, respectively. One sharp peak at 5.92 ppm indicates complete equivalence of the protons on the cyclopentadienyl rings. It is somewhat upfield from other metal-metal bonded complexes containing the group IV-B metal, such as $Cp_2ZrCH_3FeCp(CO)_2$ in which it appears at 6.25 ppm. This result also shows that the electron density on iron of $Fe(CO)_4(Cp_2ZrC_8H_{17})_2$ is higher than on Fe in other similar compounds. In the compound $Fe(CO)_4(Cp_2ZrCH_3)_2$, there are two peaks at 5.78 ppm and 0.59 ppm, assigned to cyclopentadienyl and CH_3, respectively. The integrated area is exactly 10:3.

The direct evidence for determining whether such a compound is *cis*- or *trans*-substituted around the iron at the $Fe(CO)_2^{2-}$ center could come from ^{13}C NMR spectroscopy. In order to obtain a sharp, well resolved peak in the carbonyl region, the compound should be enriched with ^{13}CO and the spectra be obtained at low temperature. The ^{13}C NMR spectrum (see Figure 2) of $Fe(CO)_4(Cp_2ZrC_8H_{17})_2$ in d_8-toluene at natural abundance shows one weak peak at 210.02 ppm at $-40°C$. On the other hand, the enriched ^{13}C NMR shows two peaks at 210.51 and 209.53 ppm at $-40°C$. The peak at 210.51 ppm and one at 209.53 ppm are assigned to the equatorial and axial carbonyl group with respect to zirconium metal complex. It is in good agreement with that of *cis*-$Fe(CO)_4(SiMe_3)_2$.[14] However, the ^{13}C NMR spectrum shows one peak at 210.10 ppm at room temperature. It may be attributable to a small energy barrier between the equatorial and axial carbonyl groups. In addition to that, there are peaks at 116, 32.5, 30.5, 14.5 ppm. The band at 116 ppm is assigned to Cp. The band at 32.5 ppm is assigned to CH_3. The other two bands are assigned to internal methylene groups.

In further studies, we are invesignating the syntheses of Fe-Ir metal-metal bonded complexes.

Acknowledgements. Auther wish to express his thanks to

professor W.M. Risen at Department of Chemistry, Brown University for technical assistance and helpful discussions and to the Korea Science and Engineering Foundation for the partial financial support.

References

1. J.R., Norton, *Acc. Chem. Res.* **12,** 139 (1979).
2. (a) E.W. Abel, F.G.A. Stone, *Q. Rev. Chem. Sco.* **24,** 498 (1970); (b) M.C. Baird, Prog. *Inorg. Chem.* **9,** 1 (1968).
3. J. Ko, *Bull, Kor. Chem. Soc.*, in press.
4. T.J. Marks and A.R. Newman, *J. Am. Chem. Soc.*, **95,** 769 (1973).
5. J. Abys and W.M. Risen, *J. Organomet. Chem.*, **204,** C5 (1981).
6. D.W. Hart and J. Schwartz, *J. Am. Chem. Soc.*, **96,** 8115 (1974).
7. K. Nakamoto, Infrared and Raman Spectra of Inorganic and Coordination Compounds, Wiley-Interscience.
8. L. Vancea and W.A.G. Graham, *Inor. Chem.*, **13,** 511 (1974).
9. (a) W. Jetz and W.A.G. Graham, *J. Organomet. Chem.*, **69,** 383 (1974); (b) A.J. Blackeney, D.L. Johnson, P.W. Donovan, and J.A. Gladysa, *Inorg, Chem.*, **20,** 4415 (1981).
10. M.R. Churchill, *Inorg. Chem.*, **6,** 185 (1967).
11. H.W. Baird and L.W. Dahl, *J. Organoment. Chem.*, **7,** 503 (1967).
12. R.K. Pomeroy and W.A.G. Graham, *J. Am. Chem. Soc.*, **94,** 274 (1972).
13. G. Ogar, personal communication
14. L. Vancea, M.J. Bennett, C.E. Jones, R.A. Smith, and W.A.G. Graham, *Inorg. Chem.*, **16,** 897 (1977).

Effect of Solvent on Some Excited States Processes of Mg- and Zn-Phthalocyanines†

Dongho Kim

Optics Lab., Korea Standards Research Institute, Daedok Science Town, Chungnam 300-31

Received June 30, 1986

The solvent coordination effect on the excited state processes of Mg(II)- and Zn(II)-phthalocyanines has been described. The triplet state of these compounds decays with mixed first and second order kinetics or mainly second order kinetics depending on the solvents used. The first order component of the rate constants decrease along with the series, dimethylsulfoxide (5-coordinated), 1-chloronaphthalene (4-coordinated) and piperidine (6-coordinated), while the second order rate constant is dependent on the diffusion rate constant of the solvents. The excited state quenching by methylviologen or p-benzoquinone is discussed. And ion recombination rate constant is given.

Introduction

The metallophthalocyanine has been the subject of many theoretical and experimental works because of their photocatalyst character and similarities to biological systems. Therefore the photophysical and photochemical behavior of the biologically important metallophthalocyanine has been investigated for a number of years.[1-4]

Despite all these efforts, not much work has been done especially about the singlet excited state and the photoexcited electron transfer reaction. Another reason for difficulty is the limitation of the solubility. Also the metallophthalocyanine interacts strongly with its environment, both via the central metal atom and peripheral functional groups. Therefore in vitro measurements must be interpreted with the solvents employed. Through the previous resonance Raman studies[5] and X-ray crystal structure work[6,7] on chlorophyll and bacteriochlorophyll, it is inferred that the central metal atom moves out of plane or in plane depending on the coordinating solvents. So the influence of different excited state energies must be considered along with the geometric effects of the solvent coordination on the photophysics of the metallophthalocyanine.

Also there is a difference in structure between the metallophthalocyanine.[1] This structural change is also expected to have an effect on the radiationless decay route in the excited singlet and triplet states (Figure 1).

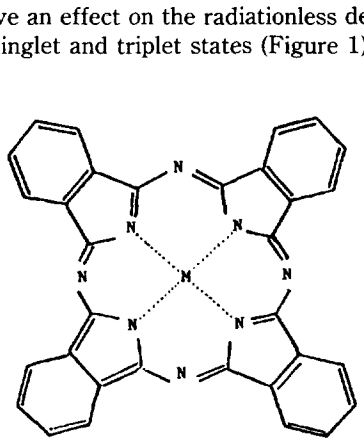

Figure 1. The structure of metallophthalocyanine. M represents the metal.

† This work was done at Washington University.

One motivation for the study of the metallophthalocyanine and related pigments is to provide fundamental information that might be useful in the development of artificial systems for photosynthetic energy coversion. We repo·t the results of the triplet state spectra, kinetics, singlet state kinetics, and electron transfer reaction in various solvents. (DMSO, piperidine, and 1-chloronaphthalene)

The state of coordination of the central metal (Zn, Mg) is either four, five, six or mixed in the solvents employed. Also we tried to see the electron transfer reaction upon the nanosecond flash photolysis of the sample in DMSO with 30 mM MV^{2+} (methylviologen) and 50 mM p-benzoquinone.

Experimental

The samples of Mg(II)-phthalocyanine(Mg-Pc) and Zn(II)-phthalocyanine(Zn-Pc) are purchased from the Eastman-Kodak chemical Co., These Samples were used without any further purification. The p-benzoquinone (Aldrich) was purified by vacuum sublimation and stored in the dark in a refrigeator. Commercially available $MVCl_2$ (Aldrich) was converted to the triflate (OTF) salt by the method of Milder *et al.*[8] in order to obtain greater solubility in organic solvents and to purify the MV^{2+}. The MV $(OTF)_2$ obtained was stored in the dark in a dessicator. The solvents (DMSO, piperidine, and 1-chloronaphthalene) are spectral grade.

Our Ruby laser system is based on a Korad Q-switched Ruby laser which delivers a 35 ns, 694 nm single pulse every minute. Figure 2 presents the block diagram of our Ruby laser system. The maximum energy of the pulse is around 1000 mJ, however for most of our experiments we reduced the energy to 150 - 200 mJ by changing the voltage of the flash lamp power supply unit.

The monitoring light was produced by a tungsten or AC xenon continuum source lamp. Right angle geometry was used to eliminate the scattering light of the laser, with two monochromators before and after the sample with bandwidth 10 nm.

A Hamamatsu 1P28A or R928 photomultiplier tube is located in a housing attached to the output slit of the monochromator after the sample. The current from the photomultiplier tube was read across a 10 K resistor into a Tektronix 468 digital storage oscilloscope (8 bit vertical resolution, 512 channels across the horizontal line, 64 channels gives the pre-triggering points) which allows for averaging signals. The termination resistance to the oscilloscope could be changed depending on the time scale. A voltage of 300 to 400 V was applied to the PMT to obtain a quiescent offset voltage of 200 mV. The voltage change was converted to absorbance change according to the formula; $\Delta A = \log_{10}(V_{off}/[V_{off}-\Delta V])$. The trigger pluse from the voltage supplier for the Pockels Cell went through the external trigger input of the oscilloscope by the BNC cable. This gives a synchronous triggering with the firing of the Ruby laser system.[9,10] The time resolution of this set-up was 15 μs. Singlet absorption spectra and picosecond time scale kinetic measurements were performed with a dual beam picosecond flash photolysis apparatus using 35 ps duration of 532 nm or 355 nm excitation pulses. The details of picosecond laser experimental system were described elsewhere.[11] The samples used were rigorously degassed by freeze-pump-thaw method (8 to 10 cycles each) on a high vacuum system (< 1 micron pressure) and sealed. The samples used in picosecond experiment are flowed. The concentration of the sample is adjusted for 0.5 A in the ground state absorption in the Q band region.

Results and Discussion

I. Ground State. Most metallophthalocyanines belong to

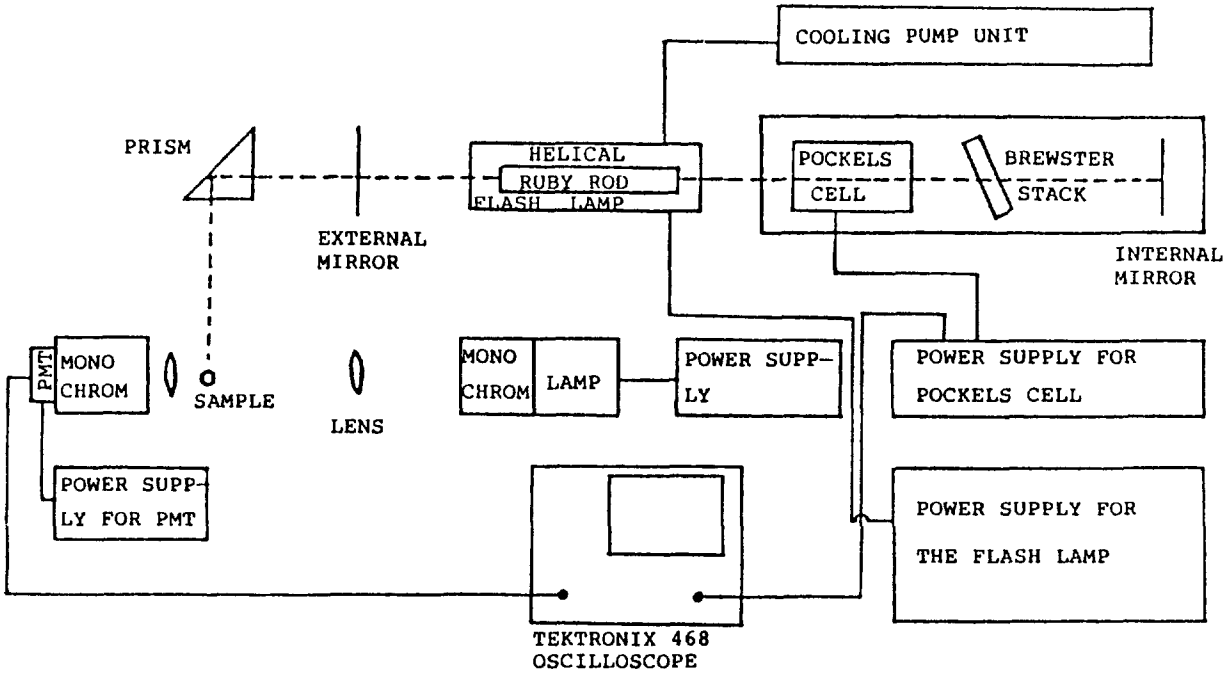

Figure 2. Block diagram of ruby laser system.

the point group D_{4h}. According to the development of Gouterman and coworkers,[1-3] the HOMO orbital is a_{1u} (π) and the next low-lying filled orbital is $a_{2u}(\pi)$. The LUMO is $e_g(\pi^*)$. Transitions from a_{1u} and a_{2u} to e_g are responsible for two $^1E_u \rightarrow {}^1A_{1g}$ (π-π^*) transitions labeled as the Q band (13,300-16,500 cm^{-1}) and Soret band (22,300-31,200 cm^{-1}) characteristic of the spectra of all metallophthalocyanine species. In addition, metallophthalocyanines exhibit one or two weaker bands near 16,500 cm^{-1} attributable to vibrational overtones of the Q band.[12] Main group (closed shell) phthalocyanines show no electronic bands other than these below about 33,000 cm^{-1}. Several metallophthalocyanines exhibit fluorescence and/or phosphorescence from the ^3E_u state associtated with the Q band. Such phosphorescence is commonly seen near 9,500-10,500 cm^{-1}. Absorption of the ^3E_u state, however, is strongly forbidden and is not observed. We have taken the ground state spectra of Mg-Pc and Zn-Pc in piperidine, DMSO and 1-chloronaphthalene. In piperidine and DMSO the Q band and Soret band are shifted to the red by 3-4 nm compared with in 1-Cl-naph. We conclude that there is a coordination change depending on solvents. Even though the separation of the peaks is too small to interpret the coordination number, it is believed that the sample makes 6-coordinated complex in piperidine and 5-coordinated complex or 5- and 6-coordinated mixture in DMSO. Our interpretation of these data comes mainly from the behavior in basic solvents of metalloporphyrins and bacteriochlorophylls.[13,14]

II. Singlet State. Because of the limited solubility of Zn-Pc in 1-Cl-naph, only the Mg-Pc* lifetime was measured in 1-Cl-naph, DMSO, and piperidine. The measured value was 5 ± 2 ns in DMSO. The error associated with this measurement is larger than the other compounds on our picosecond apparatus. In the other two solvents the lifetimes seem too long to detect within our picosecond system detection time range, and the data also looks much scattered in these two solvents. Furthermore, because the samples strongly fluoresce around the Q band region, we limited the picosecond laser work to the blue side of the Q band. That is another reason for scattering of data points in kinetics. However, we can roughly state that the coordination number of metal is important in the decay of the singlet states.

Therefore the out-of-plane metal geometry in DMSO which is expected in 5-coordination case seems to have an effect on ISC. This effect becomes even more pronounced, because there is no methine C-H bond vibrations in phthalocyanines to provide an effective route for radiationless decay. From the equation of Bowman's work,[15] the integral $\langle n|\partial H/\partial Q|$ metal $l_n^*\rangle$ is large since the electrons in the four metal-N coordination bonds in chlorophyll are strongly mixed with the p-orbitals on the nitrogen. Likewise, the integral $\langle n|H_\infty|\pi^*\rangle$ contains large one center contributions from atomic orbitals centered on the nitrogen atoms of Chl.. From these theoretical views, our data are explained qualitatively, especially shorter lifetime in DMSO.

III. Triplet State. The difference transient spectra for the formation of the triplet (Mg-Tc^T, Zn-Pc^T) were taken in 1-Cl-naph (not shown), DMSO and piperidine (Figure 3 and 4). These transient spectra are similar to those reported previously[16-18] for some other metallophthalocyanines and show the same general characteristics of a broad absorption increase around 500 nm broken by the Q_x bleaching, a bleaching of the Q_y band, and a bleaching of the Soret band

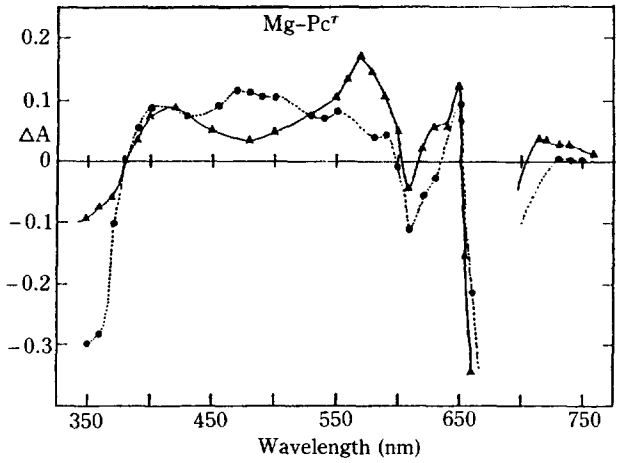

Figure 3. Transient state spectra for Mg(II) phthalocyanine in piperidine (△) at 100 μs delay and in DMSO (●) at 40 μs delay following 35 ns, 100 mJ, 694 nm ruby laser flashes.

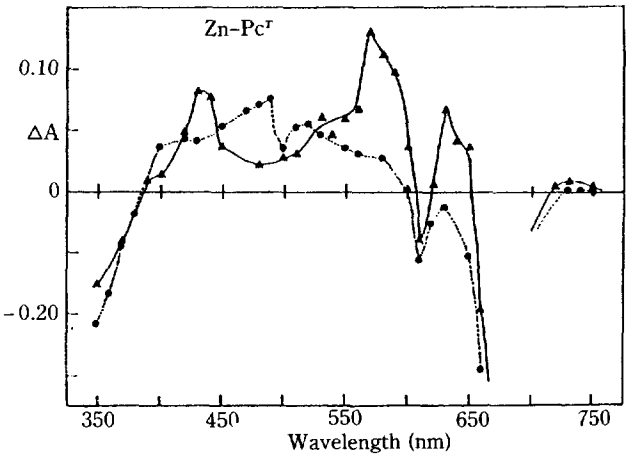

Figure 4. Transient state spectra for Zn(II) phthalocyanine in piperidine (△) at 100 μs delay and in DMSO (●) at 40 μs delay following 35 ns, 100 mJ, 694 nm ruby laser flashes.

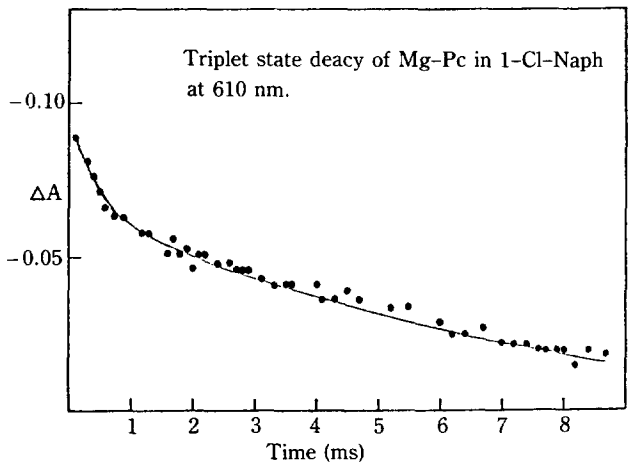

Figure 5. Triplet state decay curve for Mg(II) phthalocyanine in 1-chloronaphthalene following 35 ns, 100 mJ, 694 nm ruby laser flashes.

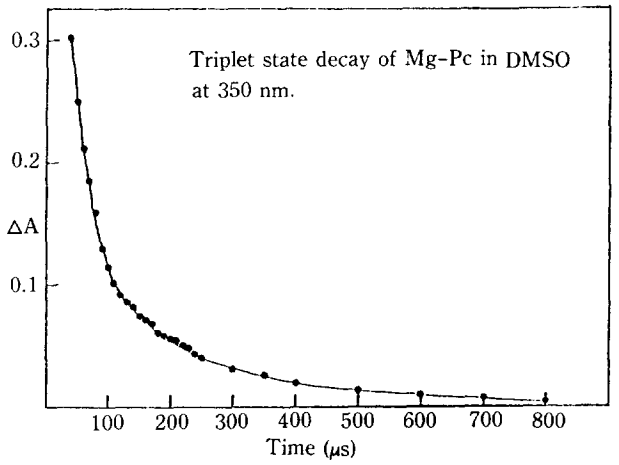

Figure 6. Triplet state decay curve for Mg(II) phthalocyanine in DMSO following 35 ns, 100 mJ, 694 nm ruby laser system.

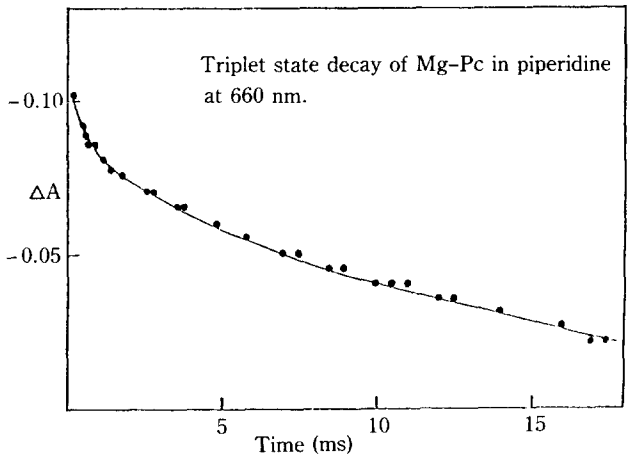

Figure 7. Triplet state decay curve for Mg(II) phthalocyanine in piperidine following 35 ns, 100 mJ, 694 nm ruby laser system.

around 360–370 nm regions. But a distinction between the triplet difference spectra in piperidine and in DMSO is the round and broad absorption around 500 nm. Also there is a discrepency in the absorption at 570 nm. The absorption change at 390–400 nm is relatively small, this fact is useful in experiments described below for the identification of the Mg-Pc and Zn-Pc cation radicals. Representative decay curves for Mg-Pc[T] in 1-chloronaphthalene, DMSO and piperidine are shown in Figures 5, 6, 7, respectively. Kinetics for the decay follow mixed first and second order kinetics or mainly second order kinetics depending on the solvents employed. The observed second order rate constant which has been multiplied by 9/5 to correct for the spin statistics associated with the formation of the singlet ground state from the interaction of two spin-one states.[13]

In Table 1, the values represent the average from several deoxygenated samples and from the decay curves at different wavelengths, mainly Q and Soret band regions. The average values of K_1 and K_2^{corr} in 1-Cl-naph and DMSO are taken by plotting first and second order mixdecay plot. However in piperidine, the second order decay processes are so dominated and the average values are taken by plotting the second order decay. From these values it is easily notified that the kinetics is dependent on the solvents employed. In going from six- or four- to five-coordinated Zn- and Mg-phthalocyanines, the Mg and Zn atom moves out of plane of macrocycle. The resulting out-of-plane metal geometry has been suggested to increase the spin-orbit coupling and hence the triplet decay rate in chlorophyll by a factor of 1.75.[15] The comparison between 6- and 4-coordinated species, it is inferred that the in-plane metal geometry is forced by two axial ligands bonding. Therefore this effect seems to decrease the spin-orbit coupling.

The other two possible factors is to shift the excited singlet state energy levels higher by the ligand coordination and to lower (n, π^*) transitions on the pyrrole nitrogens by increasing coordination numbers.[19] However these two effects are not consistent to our results, especially six-coordinated species case.

Another important mechanism of ISC is through C-H vibration but in metallophthalocyanines the carbon and hydrogen in the methine position of the macrocycle ring are replaced by nitrogen.[15] Therefore the metal position on the macrocycle ring is more important factor than in Chl *a* case. However, it is unclear to explain the enormous kinetic behavior change between solvents. Especially in piperidine the triplet state is so long-lived, its decay process mainly through the second order kinetics. In DMSO, the triplet state becomes shorter-lived, the first order decay process participate in the overall decay. Finally in 1-Cl-naph, its decay process is a intermediate case between DMSO and piperidine cases, even though the data is so scattered because of limited solubility of the sample in 1-Cl-naph. The second order rate component of the triplet state (Table 1) shows a dependence on the diffusion rate constant in a particular solvent rather than a coordination number. The diffusion rate constant was estimated from the solvent viscosity and the Debye equation $k_{diff} = 8RT/(3000\ \eta)$.[20]

Triplet yields for Mg-Pc and Zn-Pc in DMSO were measured by changing the strength of a 35 ns at 694 nm ruby laser flash. The ϕ_T was calculated from the initial slope of the absorbance change at the Soret band region. Our estimated values of ϕ_T were 6% in Mg-Pc and 4% in Zn-Pc. These lower triplet yields are consistent with previous work.[12] A natural radiative lifetime in DMSO is estimated by using our measured value of singlet lifetime $\tau_s = 5 \pm 2$ ns and an estimated fluorescence quantum yield of previous work on Mg-Pc $\phi_F = 0.6$.[12] By the equation $\phi_F = \tau_s/\tau_s^o$, the natural radiative lifetime is about 8 ns. Also a yield for $S_1 - S_o$ is calculated as $\phi_{IC} = 1 - (\phi_F + \phi_T) = 35$ % for Mg-Pc in DMSO. These calculated quantum yield values generally are in the same range as in previous work.[21]

IV. Quenching by quinone and methylviologen. Several quenchers were added to Mg-Pc and Zn-Pc to characterize the electron transfer reaction. Electron transfer reaction from Mg-Pc and Zn-Pc to p-benzoquinone or methylviologen has not been well characterized in this work. The absorption change at 390–400 nm in the triplet states of Mg-Pc and Zn-Pc is relatively small, this fact is useful for the identification of the Mg-Pc and Zn-Pc cation radicals. The quenching experiments were done only in DMSO, because of the solubility in the other solvents. Figure 8 and 9 show the spectra obtained at 30 μs delay after photolysis of Mg-Pc and Zn-Pc

Table 1. Kinetic Summary for Mg-Pc^{r} and Zn-Pc^{r} in l-Cl-naph, DMSO and Piperidine

Solvent	Coordination	k_{diff} ($M^{-1}s^{-1}$)	K_1 (s^{-1})		K_2^{corr} ($M^{-1}s^{-1}$)	
			Mg	Zn	Mg	Zn
1-Cl-Naph	4	2.2×10^{9}	$(5\pm2)\times10^{2}$	$(5\pm2)\times10^{2}$	10^{9}	10^{9}
DMSO	5	3.3×10^{9}	$(2.3\pm0.3)\times10^{3}$	$(3.7\pm0.3)\times10^{3}$	2.6×10^{9}	2.2×10^{9}
Piperidine	6	4.8×10^{9}	—	—	4.5×10^{9}	4.6×10^{9}

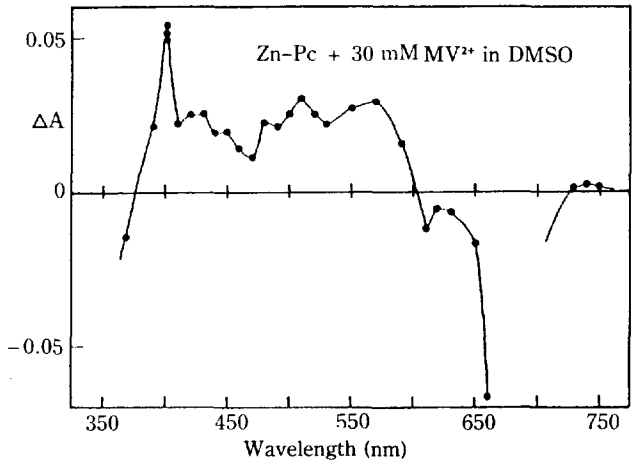

Figure 8. Transient state spectrum for Mg(II) phthalocyanine with 30 mM methylviologen in DMSO at 30 μs delay following 35 ns, 100 mJ, 694 nm ruby laser flashes.

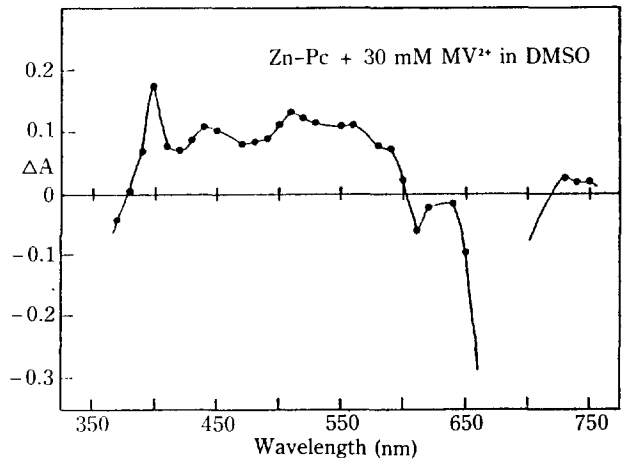

Figure 9. Transient state spectrum for Zn(II) phthalocyanine with 30 mM methylviologen in DMSO at 30 μs delay following 35 ns, 100 mJ, 694 nm ruby laser flashes.

in MV^{2+} with 35 ns flashes at 694 nm. Both the spectral and kinetic data suggest that the difference spectra are a composite of those of Mg-Pc^{r} and Mg-Pc^{+} or Zn-Pc^{r} and Zn-Pc^{+} respectively. The rather sharp absorbance increase at 400 nm is a characteristic of the viologen monocation MV^{+}, while the Mg-Pc^{+} produces the shoulder around 420 nm region.[17,18]

Table 2. Kinetic Summary for Triplet State Quenching by MV^{2+} in DMSO

Solvent	K_1 (s^{-1})		K_2^{corr} ($M^{-1}s^{-1}$)		Sample
	660 nm	400 nm	660 nm	400 nm	
DMSO	1.3×10^{4}		6×10^{9}	5×10^{8}	Mg-Pc+30 mM MV^{2+}
	2.4×10^{3}		1.6×10^{9}	3.4×10^{8}	Zn-Pc+30 mM MV^{2+}

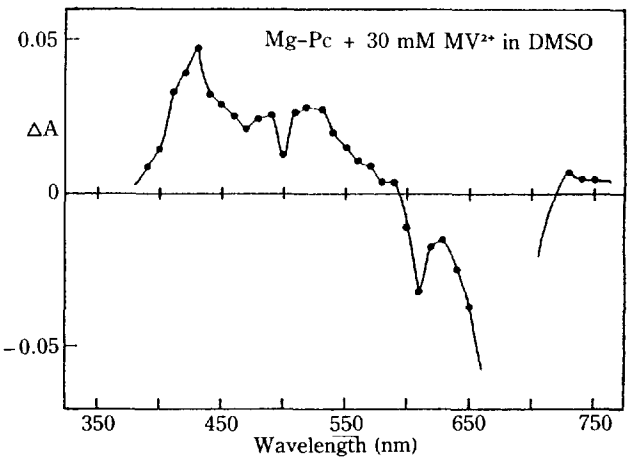

Figure 10. Transient state spectrum for Mg(II) phthalocyanine with 50 mM p-benzoquinone in DMSO at 30 μs delay following 35 ns, 100 mJ, 694 nm ruby laser flashes.

Table 2 tabulates mixdecay rate constants and second order rate constants depending on the wavelength. The rate constants taken at 400 nm represent major second order decay processes, while the rate constants at 660 nm produce the mixed first and second order decay processes. These observations stem from the fact that at 400 nm the triplet interference should be minimized, while at 660 nm the triplet species participate in overall decay processes. From these kinetic values, the recombination reactions between MV^{+} and Mg-Pc^{+} or Zn-Pc^{+} seem to be via the bimolecular processes with a rate constants a little lower than the diffusion rate constant of DMSO.[17,18] However, at 660 nm the major component is triplet state of Mg-Pc or Zn-Pc, therefore the overall processes follow the mixdecay like in DMSO without a quencher.

The similar spectra is taken with Mg-Pc in 50 mM p-benzoquinone (Figure 10), the spectrum also shows a charac-

teristic of cation radical species at 420 nm, however for Zn-Pc the electron transfer reaction experiment in p-benzoquinone could not be done because of the decomposition in the ground state.

Acknowledgement. The author thanks Prof. Dewey Holten and Mrs Christine Kirmaier for help to set up ruby laser flash photolysis system and for helpful discussions.

References

1. M. Gouterman, "The Porphyrins", ed. by D. Dolphin, Academic Press, New York, Vol. III, Chapt. 1 (1978).
2. P. Sayer, M. Gouterman, and C.R. Connell, *Acc. Chem. Res.*, **15**, 73 (1982).
3. L. Edwards, and M. Gouterman, *J. Mol. Spectrosc.*, **33**, 292 (1970)
4. A. Henriksson, B. Roos, and M. Sundbom, *Theoret. Chim. Acta.*, **27**, 303 (1972).
5. T.M. Cotton, and R.P. Van Duyne, *J. Am. Chem. Soc.*, **102**, 6020 (1981).
6. H.C. Chow, R. Serlin, and C.E. Strouse, *J. Am. Chem. Soc.*, **97**, 7230 (1975).
7. R. Serlin, H.C. Chow, and C.E. Strouse, *J. Am. Chem. Soc.*, **97**, 7237 (1975).
8. S.J. Milder, R.A. Goldbeck, D.S. Klinger and H.B. Gray, *J. Am. Chem. Soc.*, **102**, 6761 (1980).
9. J.F. Rabek, "Experimental Methods in Photochemistry and Photophysics", Part I, II, John Wiely and Sons, New York, 1982.
10. W. Koechner, "Solid State Laser Engineering", Springer Verlag, New York, 1976.
11. D. Kim, C. Kirmaier and D. Holten, *Chem. Phys.* **75**, 305 (1983).
12. P.S. Vincett, E.M. Voigt, and K.E. Rieckhoff, *J. Chem. Phys.*, **55**, 4131 (1971).
13. C.D. Tait, and D. Holten, *Photobiochem. Photobiophys.*, **6**, 201 (1983).
14. (a) A.B.P. Lever, *Adv. Inorg. Chem. Radiochem.* **7**, 27 (1965); (b) T. Tanno, D. Wohrle, M. Kaneko, and A. Yamada., *Ber. Bunsenges. Phys. Chem.* **84**, 1032 (1980).
15. M.K. Bowman, *Chem. Phys. Lett.*, **48**, 17 (1977).
16. J. McVie, R.S. Sinclair, and T.G. Truscott, *J. Chem. Soc., Faraday Transl.*, **72**, 1870 (1976).
17. T. Ohno, S. Kato, and N.N. Lichtin, *Bull. Chem. Soc. Jpn.*, **55**, 2753 (1982).
18. T. Ohno, S. Kato, A Yamada, and T. Tanno, *J. Phys. Chem.*, **87**, 775 (1983).
19. R.H. Clarke, S. Hotchandani, S.P. Jagannathan, and R.M. Leblanc, *Photochem. Photobiol.* **36**, 575 (1982).
20. A.D. Osborne, and G. Porter, *Proc. Roy. Soc.* **A284**, 9 (1965).
21. J.H. Brannon, and D. Madge, *J. Am. Chem. Soc.*, **102**, 62 (1980).

Synthesis and Characterization of New Organotin (IV)-phenylenebisdithiocarbamate Complexes

Won Ho Lee, Ok-Sang Jung, and Youn Soo Sohn*

Inorganic Chemistry Lab., Korea Advanced Institute of Science & Technology, Seoul 131

Poongzag Kim

Chemical Analysis Lab., Korea Research Institute of Chemical Technology, Dae Jeon 300-31

Received July 9, 1986

New di- and triorganotin(IV) complexes of meta- and para-phenylenebisdithiocarbamate(m- and p-pbdtc) have been synthesized and characterized by means of chemical analysis, mass spectrometry, and IR spectroscopy. The reaction of the m-pbdtc ligand with diorganotin(IV) halides resulted in 1:1 products, $R_2Sn \cdot$m-pbdtc (R = Me, Cy, n-Bu) of dimeric nature whereas the p-pbdtc ligand led to an oligomeric or polymeric structure. The pbdtc ligands were also reacted with triorganotin(IV) halides to form monomeric complexes, $(R_3Sn)_2 \cdot$pbdtc. The tin coordination chemistry of these complexes were also discussed in terms of Sn-C and Sn-S bonding modes.

Introduction

Since the first report on phenyltin(IV) dithiocarbamates in 1965[1] dithiocarbamate complexes of alkyltin(IV) or aryltin(IV) with sulphur as the donor atom have been extensively studied with a view to establish relationship between structure and biological activity. The chemical and spectroscopic studies of these complexes have revealed that tin atom can expand its coordination number above four and that dithiocarbamate ligand would be monodentate or bidentate.[2-6] In the previous study[7] diorganotin(IV) ethylenebisdithiocarbamate (ebdtc) complexes of the type $R_2Sn(S_2CNHCH_2)_2$ were synthesized in our laboratory and characterized by X-ray crystallographic study. In an effort to extend this chemistry we wish to report the syntheses and properties of the new organotin(IV) complexes of the m- and p-phenylenebisdithiocarbamate (m- and